Proc. 7th Int. Conference on Informatics in Control, Automation and Robotics,
Vol. 2, pp. 89-97, Funchal, Madeira, Portugal, (2010)

DYNAMIC MODELING AND PNEUMATIC SWITCHING CONTROL OF A SUBMERSIBLE DROGUE

Y. Han, R. A. de Callafon, J. Cortés
Department of Mechanical and Aerospace Engineering, UCSD, 9500 Gilman Drive, La Jolla, CA 92093-0411, U.S.A.
{*y3han, callafon, cortes*}*@ucsd.edu*

J. Jaffe
Scripps Institution of Oceanography, UCSD, 9500 Gilman Drive, La Jolla CA, 92093-0238, U.S.A.
jules@mpl.ucsd.edu

Keywords: Underwater robotics, Submersible drogues, Switching control.

Abstract: This paper analyzes the dynamic properties of a submersible drogue for which buoyancy control is implemented by a flexible membrane and pneumatic actuation. It is shown how a simple on/off switching algorithm tuned on the basis of depth measurements and an estimated depth velocity can be used to achieve accurate depth control with small fluctuations. The switching control makes the pneumatically controlled drogue an inherent hybrid system and conditions for contraction and stability are given for the proposed switching control algorithm. Numerical evaluation of the conditions for stability and experimental data of the switching control implemented on a pneumatic submersible drogue further demonstrates the soundness of the proposed switching control algorithm.

1 INTRODUCTION

A compelling and unanswered need in oceanography is to sample the (coastal) environment at high-resolution spatial and temporal scales than presently possible (Davis, 1991; Kunzig, 1996). Although current systems have led to many important discoveries, oceanographers would agree that many fundamental processes are presently unobservable due to the sparseness of current sampling geometries (Perry and Rudnick, 2003; Schofield and Tivey, 2004). The development of an oceanographic observatory system based on small and inexpensive buoyancy-controlled drogues that are able to perform motion control for collective oceanographic measurements could alleviate the problem of data sparseness.

One of the key requirements on (coordinated) motion is to control the individual depth of such buoyancy-controlled drogues. From a motion control point of view, alternating depth profiles can be used for motion planning purposes when using glider based propulsion (Fiorelli et al., 2003; Bhatta et al., 2005; Paley et al., 2008). On the other hand, small form factor buoyant objects can benefit from strong horizontal shear layers typically observed in shallow coastal ocean flows (Helfrich and White, 2007; Ly and Luong, 1997) to perform motion control by depth planning. Buoyancy induced motion should be done with as little control energy as possible to maximize deployment time for scientific data acquisition purposes. Requirements on energy storage are limited due to the desire of a small form factor design to simulate a free floating, low Reynolds Lagrangian-based distributed sensor system.

In this paper we will analyze the design of a single small form factor buoyancy-controlled drogue. Prototypes of buoyancy-controlled drogues are inspired by current activities at Scripps Institute of Oceanography (Colgan, 2006). Compared with these existing designs, we propose a pneumatically controlled drogue with a flexible membrane. As shown in the analysis of the dynamics, compressibility of the flexible membrane leads to an inherent unstable buoyancy equilibrium that requires very little control energy to generate alternating depth profiles. In addition, a separation of battery and pneumatic power reduces electric power and actuator requirement for motion control.

We propose a simple switching (on/off) control algorithm for the buoyancy control of the drogue. It is shown how an on/off switching algorithm tuned

This work was partially supported by NSF Award OCE-0941692.

on the basis of depth measurements and an estimated depth velocity profile can be used to achieve accurate depth control with small fluctuations. The switching control makes the pneumatically controlled drogue an inherent hybrid system (Van der Schaft and Schumacher, 2000) and a formal result on contraction and stability evaluated is given for the proposed control algorithm. The formal result on stability is evaluated numerically and both simulation and experimental data of the switching control implemented on a pneumatic submersible drogue are included in this paper to demonstrate the effectiveness of the proposed pneumatically switching buoyancy-controlled drogues.

2 ILLUSTRATION OF DESIGN CONCEPT

Previous work at Scripps Institute of Oceanography (Colgan, 2006) has illustrated the feasibility of building a standalone ball-shaped free-floating drogue vehicle. A similar, but smaller, less expensive and potentially more energy efficient concept based on a pneumatic controlled flexible membrane attached to the drogue is proposed in this paper for buoyancy control up to a depth of 150 feet. A prototype of the cylindrical shaped (1 liter in volume) membrane controlled drogue is shown in Figure 1.

(a) (b)

Figure 1: Pneumatic membrane controlled cylindrical shaped (a) drogue. Schematic inside view (b) of cylindrical shaped drogue.

Similar flexible membranes for pneumatic control of underwater drogues have also been used in ARGO floats (Gould, 2003; Gould, 2004), but at a much larger form factor. In these design concepts, the membrane actuation is primarily used for providing the buoyancy control for surfacing of the drogues. Instead, to conform to a small form factor design, we use the displaced volume under the flexible membrane for both buoyancy control and the opportunity to create alternating depth profiles that includes periodic surfacing. Due to the compressibility of the membrane, the slightest perturbation in depth will cause a change in volume and the equilibrium state of the drogue is unstable. This is beneficial for low energy periodic surfacing control. As shown in this paper, feedback control can be used to stabilize the drogue to any desired depth.

3 DYNAMIC MODELING OF PNEUMATIC DROGUE

3.1 Rigid Body Dynamics

Assuming a drag parameter d due to a drag force in water, the depth $x(t)$ of the drogue can be described by the second order differential equation

$$m\ddot{x}(t) + \text{sign}(\dot{x}(t))d\dot{x}^2(t) = F_g - F_b(t) \qquad (1)$$

where the constant rigid mass of the drogue and added mass due to displacement of fluid (Brennen, 1982) are combined in the mass parameter m. In the equation (1), F_g is the downward (constant) gravitational force

$$F_g = mg$$

and $F_b(t)$ is buoyancy force

$$F_b(t) = \rho g[V_b(t) + V]$$

determined by the fixed drogue volume V and the displaced volume $V_b(t)$ under the membrane. The constant ρ is the density of the water, which we assume to be constant at different depths. The drag parameter d is determined by the drag coefficient c_d of the drogue moving in water at a low Reynolds number and typically given by

$$d = \frac{1}{2}c_d\rho A$$

where A denotes the frontal aerial surface of the drogue. In the above equations, we consider $V_b(t)$ as a control variable to control the depth of the drogue using measurements of the depth $x(t)$.

The condition of natural buoyancy at any depth $c \geq 0$ is determined by the initial conditions $x(0) = x_0$ and $\dot{x}(0) = 0$ for the differential equation given in (1) and yields the desired (initial) volume

$$V_b(0) = V_0 = \frac{m}{\rho} - V \qquad (2)$$

for natural buoyancy. Ideally, the mass m and the volume V of the drogue should be chosen to allow for a

Water density does depend on salidity and depth, but these second order effects are neglected here

large range in $V_b(t) > 0$ for buoyancy control. However, even small changes in $V_b(t)$ suffice in generating motion of the drogue due to no-friction free body movement of the drogue floating in water.

3.2 Actuator Dynamics

Using a pneumatic mechanism to add or bleed air to effectively increase $V_b(t)$ induces additional (actuator) dynamics that needs to be taken into account in order to design a control algorithm. The displaced volume $V_b(t)$ under the membrane is a function of both the air flow, the stiffness of the membrane and the external pressure surrounding the membrane. Considering a flow $\phi(t)$ used to change the volume $V_b(t)$ under the membrane, with the ideal gas equation (Fox et al., 2004) we see that the product of the membrane pressure $P_b(t)$ and volume $V_b(t)$ can be described by

$$P_b(t)V_b(t) = \left(n_0 + \int_{\tau=0}^{t} \phi(\tau)d\tau\right) RT(t) \qquad (3)$$

where n_0 indicates the number of gas molecules for natural buoyancy at $t = 0$, R is the Boltzman constant and $T(t)$ is the gas temperature which we assume to be known (measurable) for now. Finally, we assume a linear increase of the membrane pressure $P_b(t)$ due to changes in the volume $V_b(t)$ according to

$$P_b(t) = k_m V_b(t) + P_x(t),\ P_x(t) = k_x x(t) + P_0 \qquad (4)$$

where k_m is the (linear) membrane membrane stiffness and $P_x(t)$ models the effect of the external pressure as the sum of the atmospheric pressure P_0 and the product of the depth $x(t)$ and the pressure depth constant k_x given by

$$k_x = \rho g$$

The last equation allows us to compute the unknown n_0 in (3) at time $t = 0$ for which we have natural buoyancy and $\phi(0) = 0$. With the desired initial displacement volume V_0 under the membrane given in (2), we see that at an initial depth $x(0) = x_0 > 0$

$$P_b(0) = k_m V_0 + k_x x_0 + P_0,\ \ V_0 = \frac{m}{\rho} - V$$

allowing us to compute n_0 as

$$n_0 = \frac{k_m}{RT_0} V_0^2 + \frac{k_x x_0 + P_0}{RT_0} V_0,\ \ V_0 = \frac{m}{\rho} - V$$

indicating quadratic dependency on the initial displaced volume V_0 under the membrane due to the linear membrane stiffness k_m and linear dependency due to influence of the depth dependent pressure.

To complete the analysis, we still need an equation that describes the flow $\phi(t)$. To anticipate the switching control proposed in this paper, the flow $\phi(t)$ is modulated by three different switching states: *inflate*, *deflate* or *none*. The input u can switch between the values

$$u = \begin{cases} 1 & \text{inflate} \\ -1 & \text{deflate} \\ 0 & \text{none} \end{cases}$$

can be used to distinguish between three different switching states. Using the Bernoulli equation (Fox et al., 2004) and assuming a steady incompressible flow, each state has a different flow $\phi(t)$ that is modeled via a proportional relationship with the square root of the pressure difference:

$$\phi(t) = \begin{cases} k_v^i \sqrt{P_{CO_2} - P_b(t)} & u = 1 \\ -k_v^d \sqrt{P_b(t) - P_x(t)} & u = -1 \\ 0 & u = 0 \end{cases}$$

where P_{CO_2} denotes the (constant) output pressure of the CO_2 pressure regulator and k_v^i, k_v^d denote the valve constants of respectively the add and bleed valves. If both valves are the same, then $k_v = k_v^i = k_v^d$. With the pressure relationship given in (4) we see that the gas flow $\phi(t)$ can now be modeled as

$$\phi(t) = \begin{cases} k_v^i \sqrt{P_{CO_2} - k_x x(t) - k_m V_b(t) - P_0} \\ -k_v^d \sqrt{k_m V_b(t)} \\ 0 \end{cases} \qquad (5)$$

respectively for $u = 1$, $u = -1$ and $u = 0$. As a result, membrane inflation and deflation will occur at different flow rates. Membrane inflation is determined mainly by the CO_2 pressure regulator, but pressure build up due to depth and membrane stiffness (volume) has a negative influence. For deflation it can be seen that only the membrane stiffness contributes to a desired pressure difference and is independent of depth.

3.3 Combined Dynamic Model

Combing the different equations and eliminating intermediate variables leads to a dynamic switching system described by a set of coupled non-linear and non-stiff ordinary differential equations (Hairer et al., 1993) in depth $x(t)$, volume $V_b(t)$ and gas flow $\phi(t)$ given by

$$\ddot{x}(t) = -\text{sign}(\dot{x}(t))\frac{d}{m}\dot{x}^2(t) + \frac{\rho g}{m}(V_0 - V_b(t))$$

$$k_m V_b(t)^2 + [k_x x(t) + P_0]V_b(t) = \left(n_0 + \int_{\tau=0}^{t} \phi(\tau)d\tau\right) RT(t)$$

$$\phi(t) = \begin{cases} k_v^i \sqrt{P_{CO_2} - k_x x(t) - k_m V_b(t) - P_0} & u = 1 \\ -k_v^d \sqrt{k_m V_b(t)} & u = -1 \\ 0 & u = 0 \end{cases}$$

where a summary of the meaning of the physical parameters is given in Table 2 in the Appendix of this paper. For analysis purposes, the above dynamical model is written in a short hand notation

$$\dot{z}(t) = f_u(z(t)) \tag{6}$$

where $z(t) = [x(t)\ \dot{x}(t)\ \phi(t)]^T$ combines the state variables and $f_u(z)$ for $u \in \{-1,0,1\}$ denotes the different dynamic behavior of the system as a function of the switching signal u. Simulations of the dynamics can be done along with the initial conditions

$$z(0) = \begin{bmatrix} x(0) \\ \dot{x}(0) \\ \phi(0) \end{bmatrix} = \begin{bmatrix} x_0 \\ 0 \\ 0 \end{bmatrix}$$

and the resulting initial number of gas molecules n_0 and volume given V_0 by

$$\begin{aligned} n_0 &= \frac{k_m}{RT_0} V_0^2 + \frac{k_x x_0 + P_0}{RT_0} V_0 \\ V_0 &= \frac{m}{\rho} - V \end{aligned} \tag{7}$$

It can be observed from the above equations that the membrane gas temperature T or density parameter ρ can be considered as a time or depth varying parameters that influences the dynamics of the system. The switching signal $u \in \{-1,0,1\}$ is the control input signal available to provide depth tracking and stabilization for the drogue.

4 EQUILIBRIUM AND STABILITY ANALYSIS

Equilibrium conditions for the drogue can be studied by setting the flow rate $\phi(t) = 0$ and the switching signal $u = 0$, reducing the differential equations to

$$\begin{aligned} \ddot{x}(t) = -\text{sign}(\dot{x}(t)) \frac{d}{m} \dot{x}^2(t) + \frac{\rho g}{m} (V_0 - V_b(t)) \\ k_m V_b(t)^2 + [k_x x(t) + P_0] V_b(t) = n_0 RT(t) \end{aligned} \tag{8}$$

Due to the assumptions of an ideal gas and linear membrane stiffness k_m, the volume $V_b(t)$ can be solved explicitely from the resulting quadratic equation as a function of depth $x(t)$ and temperature $T(t)$. This yields a single solution under the constraint $V_b(t) > 0$ given by

$$\begin{aligned} V_b(t) &= -\frac{1}{2k_m}[k_x x(t) + P_0] + \\ &\quad \frac{1}{2k_m}\sqrt{[k_x x(t) + P_0]^2 + 4k_m n_0 RT(t)} \end{aligned} \tag{9}$$

With $T(t) = T_0$ and both $x(t),\ V_b(t) > 0$ and n_0 given in (7) it can be seen that the solution

$$\begin{aligned} x(t) &= x_0 > 0 \\ \dot{x}(t) &= 0 \\ V_b(t) &= V_0 = \frac{m}{\rho} - V > 0 \end{aligned}$$

is a stationary point of the equation in (8) as $V_b(t)$ satisfies

$$\begin{aligned} -\frac{1}{2k_m}[k_x x_0 + P_0] + \\ \frac{1}{2k_m}\sqrt{[k_x x_0 + P_0]^2 + 4k_m^2 V_0^2 + 4k_m (k_x x_0 + P_0) V_0} = \\ -\frac{1}{2k_m}[k_x x_0 + P_0] + \\ \frac{1}{2k_m}\sqrt{(2k_m V_0 + [k_x x_0 + P_0])^2} = V_0 \end{aligned}$$

known as neutral buoyancy of the drogue at depth x_0. However, the stationary point is an unstable equilibrium as any perturbation on $x(t) = x_0$ causes an unbounded $x(t)$, physically indicating that the drogue will either surface or sink without control. Such dynamic behavior is due to the compressibility of the membrane and can be used favorably to surface without little or no control energy.

The instability of the equilibrium can be shown by considering a perturbation on the depth $x(t) > 0$ at time $t = t_p$ given by $\ddot{x}(t_p) = 0$ and $x(t_p) = x_0 + \varepsilon,\ \varepsilon > 0$. Due to this small increase in depth,

$$\begin{aligned} V_b(t_p) &= -\frac{1}{2k_m}[k_x(x_0 + \varepsilon) + P_0] + \\ &\quad \frac{1}{2k_m}\sqrt{[k_x(x_0 + \varepsilon) + P_0]^2 + 4k_m n_0 RT_0} \\ &= -\frac{1}{2k_m}[k_x x_0 + P_0] - \frac{1}{2k_m} k_x \varepsilon + \delta \end{aligned}$$

where δ is given by the expression

$$\frac{1}{2k_m}\sqrt{[k_x x_0 + P_0]^2 + 4k_m n_0 RT_0 + k_x^2 \varepsilon^2 + 2k_x (k_x x_0 + P_0)\varepsilon}$$

With $4k_m n_0 RT_0 > 0$, the strict inequality

$$\delta < \sqrt{\left(\sqrt{[k_x x_0 + P_0]^2 + 4k_m n_0 RT_0} + k_x \varepsilon\right)^2}$$

where

$$\begin{aligned} \sqrt{\left(\sqrt{[k_x x_0 + P_0]^2 + 4k_m n_0 RT_0} + k_x \varepsilon\right)^2} = \\ = \sqrt{[k_x x_0 + P_0]^2 + 4k_m n_0 RT_0} + k_x \varepsilon \end{aligned}$$

indicates that

$$\begin{aligned} V_b(t_p) < -\frac{1}{2k_m}[k_x x_0 + P_0] + \\ \frac{1}{2k_m}\sqrt{[k_x x_0 + P_0]^2 + 4k_m n_0 RT_0} = V_0 \end{aligned}$$

making the displaced volume $V_b(t_p)$ under the membrane smaller than V_0 due to $x(t_p) = x_0 + \varepsilon$. With $(V_0 - V_b(t_p)) > 0$ and $\ddot{x}(t_p) = 0$, the differential equation for $x(t)$ in (8) indicates $\dot{x}(t_p) > 0$ causing a further increase of the depth $x(t)$ for $t > t_p$. This indicates the increase of the depth $x(t)$ (sinking) and the instability of the neutral buoyancy operating point of the drogue at $x(t) = x_0$. A similar argument can be given for a perturbation $x(t_p) = x_0 - \varepsilon$ that will result in a decrease in the displaced volume $V_b(t_p)$ under the membrane, causing the drogue to surface. The stability analysis indicates that neutral buoyancy is obtained *only* at one specific (initial) depth x_0 such that $V_b(t)$ given in (9) satisfies $V_b(t) = V_0 = m/\rho - V$ to provide a buoyancy force that balances the gravitational force.

5 DEPTH SWITCHING CONTROL

Although the compressibility of the membrane can be used favorably to surface or sink the drogue without little or no control energy, a contraction or stabilization algorithm towards a target depth reference $r(t)$ must be implemented via feedback control. Due to the switching behavior of the control signal $u \in \{-1, 0, 1\}$ we can only expect to obtain depth tracking and neutral buoyancy within a user specified tolerance level α around the depth reference $r(t)$. Our objective is to design a switching control algorithm that guarantees attaining the depth region $|x(t) - r(t)| < \alpha$ from an arbitrary initial depth condition x_0.

In this paper this is achieved by simply modulating the switching signal $u \in \{-1, 0, 1\}$ on the basis of feedback information of the depth $x(t)$ and the depth velocity $\dot{x}(t)$. With a target depth $r(t) > 0$ and a γ with $0 < \alpha < \gamma$, the depth measurements are classified in three different regions that are pairwise disjoint

$$\begin{aligned} \mathcal{R}_1 &= \{x \mid \gamma < |r(t) - x|\} \\ \mathcal{R}_2 &= \{x \mid \alpha < |r(t) - x| \leq \gamma\} \\ \mathcal{R}_3 &= \{x \mid |r(t) - x| \leq \alpha\} \end{aligned} \tag{10}$$

respectively denoted by the attraction region $\mathcal{R}_1$, the stabilization region $\mathcal{R}_2$ and the tolerance region $\mathcal{R}_3$. We will first summarize the proposed switching control algorithm. Subsequently we provide a proposition that shows how contraction to a specific depth region can be obtained.

Algorithm 1. *Let $\mathcal{R}_j,\ j = 1,2,3$ be the depth region defined in (10) where $0 < \alpha < \gamma$ and consider the maximum drogue velocities β_j for each region $\mathcal{R}_j$ where $\beta_3 \leq \beta_2 \leq \beta_1$ and let*

$$\sigma = sign(r(t) - x(t)) \in \{-1, 1\}$$

Default, the switching signal $u = 0$ but will be either $u = 1$ (add air to increase the volume $V_b(t)$) or $u = -1$ (bleed air to reduce $V_b(t)$) according to the following rules:

1. *If $x(t) \in \mathcal{R}_1$, consider the two situations:*
   a. *If $|\dot{x}(t)| \leq \beta_1$ then $u = -\sigma$ (increase depth velocity)*
   b. *If $\sigma \cdot \dot{x}(t) < 0$ then $u = -\sigma$ (velocity in wrong direction, increase/decrease depth velocity directly)*
2. *If $x(t) \in \mathcal{R}_2$, consider the two situations:*
   a. *If $|\dot{x}(t)| > \beta_2$ and $\sigma \cdot \dot{x}(t) > 0$ then $u = \sigma$ (decrease velocity)*
   b. *If $\sigma \cdot \dot{x}(t) < 0$ then $u = -\sigma$ (velocity in wrong direction, increase/decrease depth velocity directly)*
3. *If $x(t) \in \mathcal{R}_3$ and $|\dot{x}(t)| > \beta_3$ then $u = sign\{\dot{x}(t)\}$ (chatter input signal to achieve velocity bound)*

As can be seen from the above algorithm, each region $\mathcal{R}_j,\ j = 1,2,3$ has specific bounds β_j on the depth velocity $\dot{x}(t)$ that determines the modulating of the switching signal $u \in \{-1, 0, 1\}$. The attraction region $\mathcal{R}_1$ is used to give the drogue the right velocity with a maximum of β_1 to attract it in the stabilization region $\mathcal{R}_2$. When the drogue enters the region $\mathcal{R}_2$, the velocity is reduced to β_2 to avoid abrupt entering and exiting of $\mathcal{R}_2$ and providing an entering velocity of β_2 for the tolerance region $\mathcal{R}_3$. Obviously, the choice of β_2 is closely related to the size of γ. As soon as the drogue enter the tolerance region $\mathcal{R}_3$ the control can be turned off by choosing $\beta_3 = \beta_2$ as the entering velocity will be β_2. Choosing $\beta_3 < \beta_2$ allows an additional reduction of drogue velocity within the tolerance region at the price of a chattering control signal.

The proposed switching control in Algorithm 1 is motivated by the need to dampen the (unstable) rigid body motion of the drogue and maintain neutral buoyancy. The proposed algorithm is basically a Proportional and Derivative (PD) control architecture with specific level sets for position $x(t)$ and velocity $\dot{x}(t)$ measurements. It should be observed that feedback information on $x(t)$ and $\dot{x}(t)$ is required to implement the proposed control algorithm. However, $\dot{x}(t)$ can be approximated by discrete-time sampling and filtering of the depth $x(t)$, allowing a discrete-time implementation of the switching control algorithm based on depth measurements only.

6 HYBRID STABILITY ANALYSIS

For the analysis of the proposed switching control algorithm, the framework of hybrid systems analysis (Van der Schaft and Schumacher, 2000; Liberzon, 2003; Goebel et al., 2009) can be used to prove stability properties of the resulting control system. Based on the switching control law proposed in Algorithm 1, the behavior of the drogue is modeled as a hybrid system with three different modes corresponding to *inflation* for $u = 1$, *deflation* for $u = -1$, and a *neutral* mode for $u = 0$.

Each mode has its active region and these regions share switching surfaces with each other. The transition between modes occurs when the system trajectory crosses these switching surfaces. In this paper, a multiple Lyapunov functions based parameter dependent switching strategy is used to investigate the stability of the proposed switching control algorithm for the buoyancy control of the drogue.

In order to establish an active region for each actuator dynamic mode, three Lyapunov functions V_u, $u \in \{-1,0,1\}$ must be defined. The three quadratic Lyapunov functions V_u are defined as follows:

$$\begin{aligned} V_1 &= \frac{1}{2}(-(x-r)-10\dot{x}+\phi)^2 \quad \text{inflation} \\ V_{-1} &= \frac{1}{2}(-(x-r)-10\dot{x}+\phi)^2 \quad \text{deflation} \\ V_0 &= \frac{1}{2}(x-r)^2+\frac{1}{20}\dot{x}^2 \quad \text{neutral} \end{aligned} \tag{11}$$

Subsequently, the stability analysis is based on a theorem in (Branicky, 1998) on Lyapunov stability of switched and hybrid systems and summarized in the following result for the switched hybrid system considered in this paper.

Proposition 1. *Consider the system $\dot{z}(t) = f_u(z(t))$ in (6) and let V_u be the Lyapunov functions given in (11) for $u \in \{-1,0,1\}$. Let $L_{f_u}V_u$ be the Lie derivative of V_u along the vector field spanned by the subsystem $f_u(\cdot)$. The origin of the system is asymptotically stable if the following two conditions are satisfied*

$$\begin{aligned} &(a) \quad L_{f_u}V_u < 0 \text{ for each } u \in \{-1,0,1\} \\ &(b) \quad V_u \text{ is nonincreasing along switching} \\ &\qquad \text{times on the } u\text{th system } \dot{z}(t) = f_u(z(t)) \end{aligned} \tag{12}$$

In this paper we use numerical analysis to verify the two conditions (12) in Proposition 1. It can be verified that each Lyapunov function V_u for $u \in \{-1,0,1\}$ in (11) is positive definite over its active region characterized by $L_{f_u}V_u < 0$. To characterize (12) over the three dimensional state vector $z = [x\ \dot{x}\ \phi]^T$ Lyapunov analysis is conducted by varying ϕ in the admissible range. This can be done as ϕ is not used directly in the switching control of Algorithm 1. Numerical evaluation of (12) for different values of ϕ is done using a non-stiff differential equation solver (Cooper, 2004) and implemented via `ode45` in Matlab.

For the inflation mode, $L_{f_1}V_1$ for $\phi = 0$ is plotted in Figure 2 and the active region for which (12) holds is separated by a dashed line, whereas the arrows indicate a decreasing value of V_1. If ϕ is varied, the whole solution surface moves through the ϕ-axis (perpendicular to $x - \dot{x}$ plane) resulting in the shift of the active region along the $\dot{x}$-axis. The same analysis can be done for other modes. A similar plot is created for the deflation mode where $L_{f_{-1}}V_{-1}$ for $\phi = 0$ is plotted in Figure 3 and the neutral mode where $L_{f_0}V_0$ for $\phi = 0$ is plotted in Figure 4.

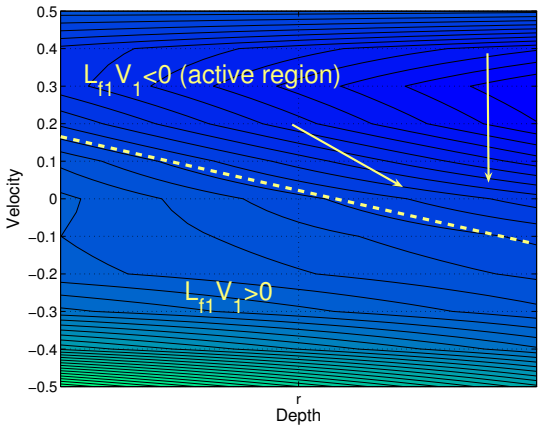

Figure 2: The active region of the inflation mode. The arrows indicate the allowable direction of solution trajectory. In inflation mode, the solution trajectory always follows this allowable direction.

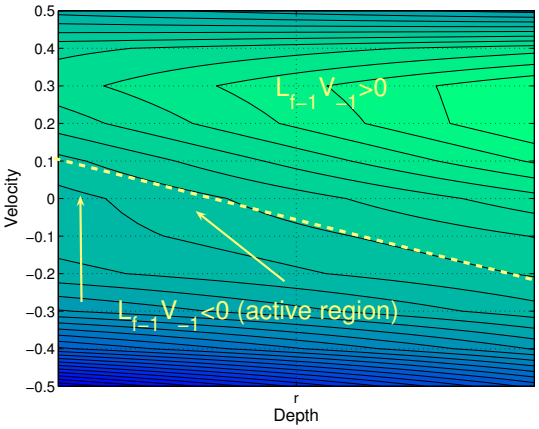

Figure 3: The active region of the deflation mode. The arrows indicate the allowable direction of solution trajectory. In deflation mode, the solution trajectory always follows this allowable direction.

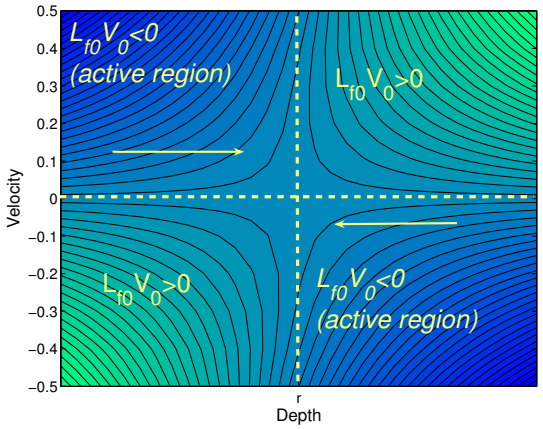

Figure 4: The active region of the neutral mode. The arrows indicate the allowable direction of solution trajectory. In neutral mode, the solution trajectory always follows this allowable direction.

Table 1: Numeric parameters of dynamic drogue model for non-linear simulation of switching control algorithm.

symbol	value	units
V	10^{-3}	m^3
m	1.5	kg
d	30	$N/m^2/s^2$
ρ	$1.03 \cdot 10^3$	kg/m^3
g	9.81	m/s^2
k_m	$5 \cdot 10^8$	Pa/m^3 or N/m^5
T_0	288	K
R	8.314472	$(m^3Pa)/(K\ mol)$
k_a	10^{-4}	$mol/\sqrt{Pa}$
k_b	10^{-4}	$mol/\sqrt{Pa}$
P_{CO_2}	10^6	Pa or N/m^2
P_0	10^5	Pa or N/m^2
x_0	10	m

Based on these figures, the existence of a stability region characterized by (12) can be verified. Therefore, the proposed hybrid control strategy using the active regions and switching surfaces stabilizes the drogue system.

7 SIMULATION RESULTS

To illustrate the performance of the switching control in Algorithm 1, the controlled dynamic behavior of a model of a buoyancy controlled submersible drogue is simulated. The model is based on the set of coupled non-linear differential equations given in (6) and based on the numerical parameters listed in Table 1. A summary of the meaning of the physical parameters is given in Table 2 in the Appendix of this paper.

Using the switching control summarized in Algorithm 1 with the regions of (10) based on a depth tolerance $\alpha = 0.5$m and a stabilization region specified by $\gamma = 2\alpha = 1$m and a maximum velocity $\beta_1 = 0.3$m/s in region $\mathcal{R}_1$ and a maximum velocity $\beta_2 = \beta_3 = 0.1$m/s in region $\mathcal{R}_2$ and $\mathcal{R}_3$, the performance of the switching control algorithm can be evaluated by the simulation results depicted in Figure 5. The results were computed by numerically solving the non-stiff differential equations of the ODE's of the model of the drogue using an implementation of the explicit Runge-Kutta (4,5) pair implemented in `ode45` in Matlab (Shampine and Reichelt, 1997).

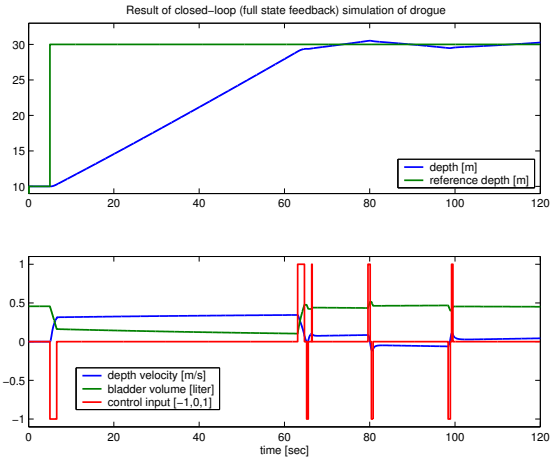

Figure 5: Simulation results of switching control Algorithm 1 with $\alpha = 0.5$m, $\gamma = 1$m, $\beta_1 = 0.3$m/s and $\beta_2 = \beta_3 = 0.1$m/s when the target depth references $r(t)$ changes from 10m to 30m at $t = 5$sec. The numerical values for the drogue model used during this simulation are listed in Table 1.

During the simulation the target depth $r(t)$ of $10m$, for which the drogue is initially neutrally buoyant, is changed to $30m$ at $t = 5$sec. It can be seen from the simulation results in Figure 5 that the drogue stays within approximately $\pm\alpha$m of the a constant target depth, whereas a change to a different target depth is accomplished with a maximum speed of $\beta_1 = 0.3$m/s and only requires a few switches of the control signal u. During steady state operation only very short actuation of either the "add" ($u = 1$) or "bleed" ($u = -1$) valves are used to maintain depth within the specified tolerance region α and stabilization region γ. The simulation confirms the hybrid stabilization results.

8 EXPERIMENTAL RESULTS

In an initial testing phase, the proposed control algorithm was implemented on the pneumatic membrane controlled cylindrical shaped drogue depicted in Figure 1(a). The drogue design uses an internally stored standard compressed 16 gram CO_2 cartridge with a regulator assembly to change the displaced volume under the latex or neopropene membrane via two small form factor Numatics series solenoid valves. One valve is used for inflating the membrane, the other valve is to bleed the CO_2 from the membrane.

The electrical components are powered by three 3.7Volt, 2700mAH Li-Ion batteries. A model 85 Ultra Stable Pressure Sensor is used for depth measurements measured by a 10bit AD converter on a Microsystems PIC18F4620 microprocessor.

The embedded control of the pneumatically controlled drogue only uses depth measurements $x(t)$ sampled at 10Hz and depth velocity estimates $v(t)$ are obtained via

$$v(t) = \frac{x_f(t) - x_f(t)}{\Delta_t}, \; x_f(t) = F(q)x(t)$$

where $F(q)$ is a second order Butterworth filter with a normalized cut-off frequency of 0.1 (1Hz). Both the depth measurements $x(t)$ and the control signal $u(t)$ as a function of the discrete-time t were saved for validation purposes and the results of the experimental work is summarized in Figure 6.

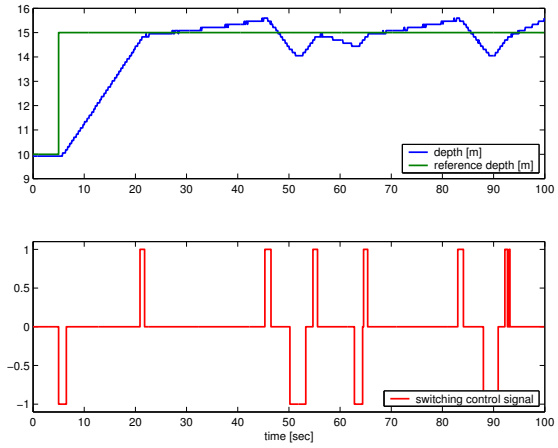

Figure 6: Preliminary experimental results of switching control Algorithm 1 with $\alpha = 0.5m$, $\gamma = 1$, $\beta_1 = 0.3$m/s and $\beta_2 = \beta_3 = 0.2$m/s applied to the pneumatic membrane controlled cylindrical shaped drogue depicted in Figure 1(a). The target depth references $r(t)$ changes from 10m to 15m at $t = 5$sec.

The experimental results confirm the stability of the control algorithm for the pneumatic membrane cylindrical shaped drogue even for the discrete-time implementation of the algorithm. The slightly larger values of β_2 and β_3, chosen due to the noise levels on the estimated velocity $v(t)$, cause larger velocity swings in the stabilization and tolerance region. Moreover the quantization effects of the depth measurements based on a 10bit AD converter also cause resolution limiations on the velocity estimate. It can be seen that a larger value for β_2 requires more switching for stabilization. Tuning of the controller parameters α, γ, β_1 and β_2 can be used to further improve the controller performance.

9 CONCLUSIONS

The dynamic properties of a submersible drogue for which buoyancy control is implemented by a flexible membrane can be described by a set of coupled nonlinear and non-stiff ordinary differential equations. It is shown that the compressibility of the membrane leads to an dynamically unstable dynamical system in terms of the depth, which can be used favorably to surface or sink the drogue without little or no control energy.

The instability does require a contraction or stabilization algorithm to maintain a target depth reference. In this paper it is shown that a simple pneumatic on/off switching control algorithm in which compressed CO_2 is either added or extracted from the membrane actuator on the basis of three different and pairwise disjoint depth regions can be used to stabilize the depth positioning of the drogue.

The switching control algorithm leads to a hybrid dynamical system, for which stability analysis results are summarized in the paper. Numerical evaluation of the stability conditions reveal that the proposed on/off switching control algorithm leads to a stabilized buoyancy-controlled drogue. Both simulation and experimental studies indicate stability properties and depth tracking performance within a specified tolerance levels.

REFERENCES

Bhatta, P., Fiorelli, E., Lekien, F., Leonard, N. E., Paley, D., Zhang, F., Bachmayer, R., Davis, R. E., Fratantoni, D. M., and Sepulchre, R. (2005). Coordination of an underwater glider fleet for adaptive ocean sampling. In *International Workshop on Underwater Robotics, Int. Advanced Robotics Programmed (IARP)*, Genoa, Italy.

Branicky, M. (1998). Multiple Lyapunov functions and other analysis tools for switched and hybrid systems.

IEEE Transactions on Automatic Control, 43:475–482.

Brennen, C. (1982). A review of added mass and fluid inertial forces. Technical Report CR82.010, Naval Civil Engineering Laboratory.

Colgan, C. (2006). Underwater laser shows. *Explorations, Scripps Institution of Oceanograhpy*, 12:20–27.

Cooper, J. (2004). *An Introduction to Ordinary Differential Equations*. Cambridge University Press.

Davis, R. (1991). Observing the general circulation with floats. *Deep-Sea Research*, 38:531–571.

Fiorelli, E., Bhatta, P., Leonard, N. E., and Shulman, I. (2003). Adaptive sampling using feedback control of an autonomous underwater glider fleet. In *Proceedings 13th International Symposium on Unmanned Untethered Submersible Technology*, Durham, NH.

Fox, R., McDonald, A., and Pritchard, P. (2004). *Introduction to Fluid Mechanics*. John Wiley & Sons Inc., Hoboken, NJ, U.S.A.

Goebel, R., Sanfelice, R. G., and Teel, A. R. (2009). Hybrid dynamical systems. *IEEE Control Systems Magazine*, 29:283.

Gould, J. (2004). Argo profiling floats bring new era of in situ ocean observations. *Earth and Ocean Sciences*, 85(11).

Gould, W. J. (2003). WOCE and TOGA - the foundations of the global ocean observing system. *Oceanography, Special Issue on Ocean Observations*, 16(4):24–30.

Hairer, E., Nørsett, S. P., and Wanner, G. (1993). *Solving Ordinary Differential Equations I: Nonstiff Problems*. Springer Verlag, Berlin.

Helfrich, K. and White, B. (2007). Rapid gravitational adjustment of a horizontal shear layer. In *American Physical Society, 60th Annual Meeting of the Divison of Fluid Dynamics*.

Kunzig, R. (1996). A thousand diving robots. *Dis. Mag.*, 17:60–63.

Liberzon, D. (2003). *Switching in Systems and Control*. Systems & Control: Foundations and Applications series. Birkhauser, Boston.

Ly, L. N. and Luong, P. (1997). A mathematical coastal ocean circulation system with breaking waves and numerical grid generation. *Applied Mathematical Modelling*, 21:633–641.

Paley, D., Zhang, F., and Leonard, N. E. (2008). Cooperative control for ocean sampling: The glider coordinated control system. *IEEE Transactions on Control Systems Technology*, 16:735–744.

Perry, M. and Rudnick, D. (2003). Observing the ocean with autonomous and lagrangian platforms and sensors (ALPS): The role of ALPS in sustained ocean observing systems. *Oceanography*, 4:31–36.

Schofield, O. and Tivey, M. (2004). Building a window to the sea: Ocean research interactive observatory networks (ORION). *Oceanography*, pages 113–120.

Shampine, L. F. and Reichelt, M. W. (1997). The Matlab ODE suite. *SIAM Journal on Scientific Computing*, 18:1–22.

Van der Schaft, A. and Schumacher, H. (2000). *An Introduction to Hybrid Dynamical Systems*. Lecture Notes in Control and Information Sciences 251, Springer-Verlag.

APPENDIX

Table 2 summarizes the symbols use in the derivation of the dynamical model of the drogue in Section 3.3.

Table 2: Summary of symbolic parameters of dynamic drogue model.

symbol	meaning
V	volume of drogue
m	mass of drogue
d	drag parameter in water
ρ	density of sea water
g	gravitational constant
k_m	linear membrane stiffness
T_0	temperature of water
R	gas constant
k_a	'add air' valve constant
k_b	'bleed air' valve constant
P_{CO_2}	regulated CO_2 pressure
P_0	atmospheric pressure
x_0	depth for neutral buoyancy